ARTICLE IN PRESS
JID: ACTBIO [m5G;June 5, 2021;9:2]
Acta Biomaterialia xxx (xxxx) xxx

Contents lists available at ScienceDirect

Acta Biomaterialia

journal homepage: www.elsevier.com/locate/actbio

Full length article

Strains induced in the vagina by smooth muscle contractions

Alyssa Huntington[a], Steven D. Abramowitch[b], Pamela A. Moalli[c], Raffaella De Vita[a,*]

[a] STRETCH Lab, Department of Biomedical Engineering and Mechanics, Virginia Tech, Blacksburg, VA, 24061, USA
[b] Translational Biomechanics Lab, Department of Bioengineering, University of Pittsburgh, Benedum Hall, 3700 O'Hara Street, Pittsburgh, PA, 15213, USA
[c] Department of Obstetrics, Gynecology and Reproductive Sciences, University of Pittsburgh School of Medicine, Magee-Womens Research Institute, 204 Craft Ave, Pittsburgh, PA, 15213, USA

ARTICLE INFO

Article history:
Received 15 March 2021
Revised 12 May 2021
Accepted 13 May 2021
Available online xxx

Keywords:
Vagina
Isometric contraction
Biaxial testing
Strain
Contractility

ABSTRACT

The ability of the vagina to contract gives rise to a set of active mechanical properties that contribute to the complex function of this organ *in-vivo*. Regional differences in the morphology of the vagina have been long recognized, but the large heterogeneous deformations that the vagina experiences during contractions have never been quantified. Furthermore, there is no consensus regarding differences in contractility along the two primary anatomical directions of the vagina: the longitudinal direction (LD) and the circumferential direction (CD). In this study, square vaginal specimens from healthy virgin rats ($n = 15$) were subjected to isometric planar biaxial tests at four equi-biaxial stretches of 1.0, 1.1, 1.2, and 1.3. Contractions were induced at each stretch by a high concentration potassium solution. The digital image correlation method was used to perform full-field strain measurements during contractions. The vagina was found to undergo significantly higher compressive strains, tensile strains, and contractile forces along the LD than along the CD during contractions. Specifically, when computed over all the applied equi-biaxial stretches, mean (± std. dev.) absolute maximum compressive strains were -(13.43 ± 1.56)% along the LD and -(3.19 ± 0.25)% along the CD, mean absolute maximum tensile strains were (10.92 ± 1.73)% along the LD and (3.62 ± 0.57)% along the CD, and mean maximum contractile forces were 6.24 ± 0.55 mN along the LD and 3.35 ± 0.56 mN along the CD. Moreover, the vaginal tissue appeared to undergo compression in the proximal region and tension in the distal region while kept at constant equi-biaxial stretches. The active mechanical properties of the healthy vagina need to be fully investigated so that detrimental alterations in vaginal contractility, such as those caused by pelvic floor disorders and current treatment strategies, can be prevented.

Statement of significance

Contractile forces of the vagina have been measured by several investigators using uniaxial tensile testing methods. Unlike previous studies, in this study planar-biaxial tests of vaginal specimens were performed while the full-field strains of the vagina, as induced by smooth muscle contraction, were measured. The vagina was found to generate significantly larger contractile strains and forces in the longitudinal direction than in the circumferential direction. Knowledge of the contractile mechanics of the healthy vagina is essential to understand the detrimental effects that pelvic organ prolapse and the use of surgical meshes have on the functionality of smooth muscle in the vagina.

1. Introduction

The vagina is a highly dynamic tubular organ that undergoes tremendous changes. Long-term changes are mainly hormone-mediated, occurring during puberty, pregnancy, and menopause. During puberty, the overall size of the vagina increases, the vaginal fornices develop, and the inner layer of the organ, the epithelium, becomes thicker and stratifies. With pregnancy, the connective tissue of the vagina relaxes and the muscle fibers thicken but, after delivery, the vagina returns to its normal shape. Through menopause and older age, the vagina becomes thinner and frailer, losing lubrication [1]. Short-term changes such as vaginal tenting

* Corresponding author.
E-mail address: devita@vt.edu (R. De Vita)

or ballooning during intercourse also occur, with the vagina becoming longer and wider [2].

Within the pelvic cavity, the vagina is kept in place and supported by a complex network of connective tissues. In a relaxed state, the posterior and anterior walls of the human vagina are collapsed by the surrounding tissues and organs and the cross-section of the vaginal lumen has a H or W shape [3,4]. The inner walls of the vagina are covered by folds, called *rugae*, that allow the organ to distend and stretch under pressure. Throughout daily life, the vagina experiences deformations in response to the forces exerted by the surrounding connective tissues and changes in intra-abdominal pressure. The relaxation and contraction of vaginal smooth muscle (VaSM) likely plays a major role in modulating the internal stresses brought about by these deformations.

Contractions of the vagina are generated by the muscularis. The muscularis is typically described as having two layers, one with muscle oriented along the longitudinal direction (LD) and one with muscle oriented along the circumferential direction (CD); however these layers are not always easily distinguished from each other across the whole muscularis [5,6]. Still, having muscle oriented along both the LD and CD gives the vagina the ability to contract along each of these directions. The differences in the forces that the vagina generates during contractions in the LD and CD have been studied to some extent by performing *ex vivo* uniaxial tests [7,8], planar biaxial tests [9], and inflation-extension tests [10] as summarized in Fig. 1. While the planar biaxial and inflation-extension tests showed that the vagina generates higher contractile forces along the LD than the CD in response to potassium chloride (KCl), uniaxial tests yielded conflicting results, suggesting the need for additional investigations on the direction-dependent contractions of the vagina. Furthermore, the contractility of muscle with respect to region within an organ sheds light on the mechanisms by which that organ functions. For example, the contractility of the porcine bladder was found to be relatively homogeneous, indicating that it expels urine through uniform contractions across the entire organ [11], whereas the contractility of the pig stomach was found to be highly heterogeneous, corresponding to zones of the stomach that process food in different ways [12]. In the vagina, the regional variation of muscle contractility, as well as the functional implications of said variation, is still unclear. Muscle within the distal vagina, which has been found to have a sphincter-like structure, likely provides mechanical support to the vaginal orifice [7,13]. Muscle in the proximal vagina, which has been described as being more compact and neatly organized than muscle in the distal region [13,14], may be important for vaginal lengthening during sexual arousal [5]. While vaginal contractile forces have been measured using various testing methods and animal models, as recently reviewed by some of the authors, there are currently no published studies that report the large strains that are experienced by the vagina due to VaSM contractions [15]. Quantifying the deformations of the vagina induced by VaSM contractions is essential for elucidating the etiology of pelvic floor disorders (PFDs) and developing better treatment methods.

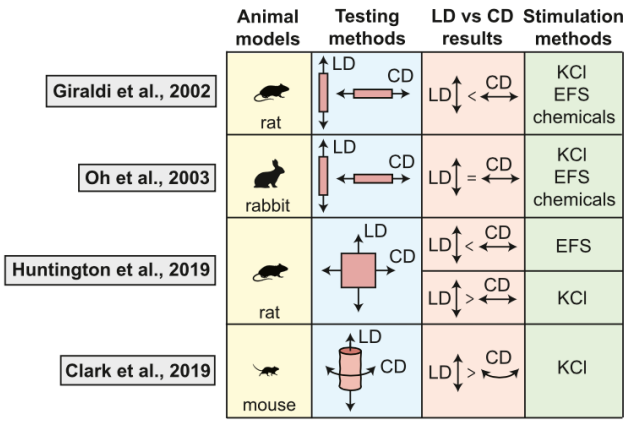

Fig. 1. Summary of published uniaxial and biaxial studies examining differences in contractile forces of the vagina in the longitudinal direction (LD) and circumferential direction (CD). KCl: potassium chloride, EFS: electrical field stimulation. Using uniaxial tests, Giraldi et al. [7] observed larger contractile forces along the CD than the LD in the rat vagina, and Oh et al. [8] observed similar contractile

Almost 24% of women in the United States develop symptoms of at least one pelvic floor disorder, and this proportion increases to nearly 50% for women over the age of 80 [16]. Pelvic organ prolapse (POP), characterized by the descent of the uterus, bladder, or rectum into the vaginal canal, is one of the most common PFDs. It is estimated that women have a lifetime risk of 12.6% of undergoing surgery to treat POP [17]. While the etiology of POP is likely multifactorial, alterations of the VaSM have been identified with the development of POP. In women with prolapse, fractional area of smooth muscle within the vaginal wall significantly decreases [6,18–21], cell apoptosis increases [21], and expression of contractile proteins is altered [22]. Together, these studies provide strong evidence that the development of POP and the reduction of VaSM content and functionality are correlated, though it remains unclear whether such changes in VaSM are among the causes or, rather, the effects of POP.

Current treatment options for POP mainly include physical therapy, the use of pessaries, and surgery. While conservative treatment is prioritized, women with severe symptoms often opt for surgical intervention. However, surgical procedures for POP have low success rates, high prolapse recurrence rates, and several risks. Recently, transvaginal surgical mesh implants for POP have fallen out of common use due to a lack of evidence of their safety and efficacy [23]. Complications associated with surgical mesh devices are due, in part, to material mismatch between the devices and the native tissues with which the devices become integrated. Among the negative effects of surgical meshes is a degeneration of VaSM, as identified by several investigators [24–28]. Mesh-treated vaginas have thinner muscle layers [25,28], smaller muscle bundles [26], as well as lower contractile force generation capabilities [24–28] than control vaginas. Muscle degeneration in response to meshes may be a result of the stress shielding that occurs between the stiff mesh device and the soft vaginal tissue [29]. The quantification of the strains that the vagina undergoes in-vivo, including those caused by VaSM contraction alone, is an essential step for the development of implantable mesh devices that can successfully interact and deform with the host organ.

In this study, we sought to quantify regional differences in contractility of the vagina with respect to the main anatomical directions, the LD and CD. We hypothesized that the contractile strains experienced by the vagina would be highly heterogeneous, and that higher magnitudes of strains would occur along the direction that generated stronger contractile forces. Toward this end, square specimens of rat vaginal tissue, with sides oriented along the LD and CD, were subjected to isometric biaxial tests, while measuring, for the first time, two-dimensional full field contractile strains and contractile forces. Knowledge about the contractions of the

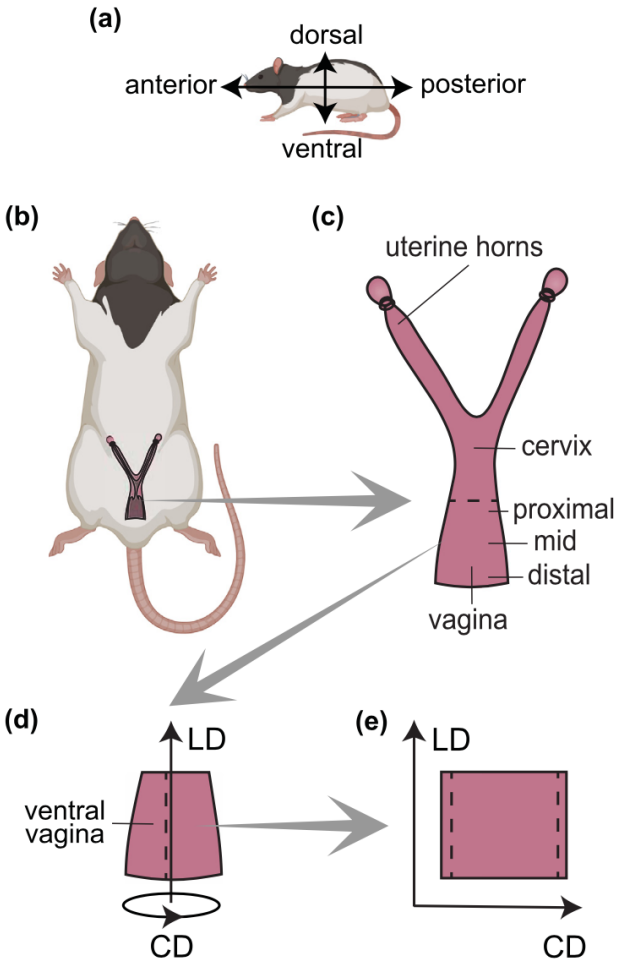

Fig. 2. (a) Anatomical orientations and directions in the rat. (b) Location of reproductive organs in the rat (ventral side). (c) Location of proximal, mid, and distal vagina relative to cervix and uterine horns. (d) Cut placed on the ventral vagina with represented LD and CD. (d) Square vaginal specimen with sides parallel to LD and CD.

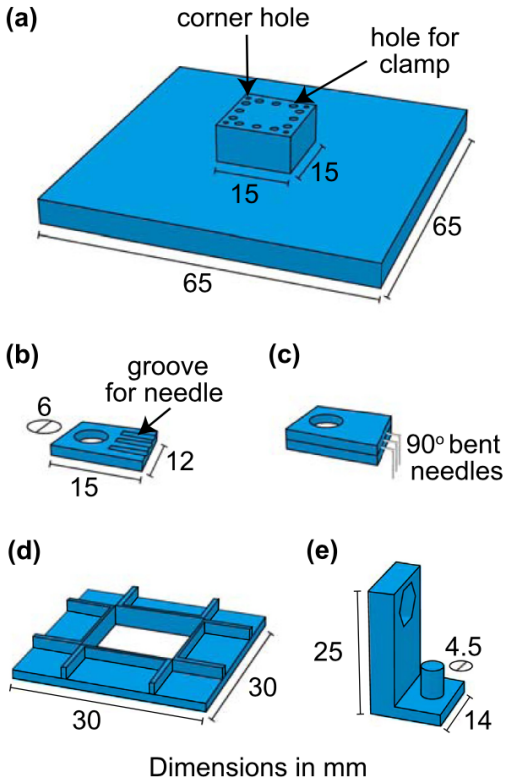

Fig. 3. Components of the clamping/mounting system with important dimensions in mm. (a) Flat base with a central raised square platform to hold the specimen for clamping. (b) One of the eight rectangular blocks used to fabricate the four clamps. (c) One clamp made of two rectangular blocks as shown in (b) that were superglued together with three protruding 90° bent needles. (d) Frame with rails to keep the specimens and clamps aligned during dismounting from the clamping platform and mounting on to the biaxial testing apparatus. (e) One of the four brackets that connected the actuators of the biaxial testing apparatus to the clamps.

2. Methods

2.1. Specimen preparation

Adult female Long-Evans rats ($n = 15$) aged between 12 and 14 weeks (Envigo, Indianapolis, IN) were euthanized via decapitation in accordance with a protocol approved by the Institutional Animal Care and Use Committee (IACUC) at Virginia Tech. The vagina was carefully separated from the rectum and connective tissues around its circumference using small dissection scissors starting at the introitus and moving anteriorly (Fig. 2(a)) until the pubic bone was reached. At this point the pelvic cavity was opened for better visibility of the reproductive tract (Fig. 2(b), (c)). The pubic bone was cut using bone cutters and pulled open with forceps after its connections to the vagina had been severed. The cervix was identified by its lighter color and by its firm texture. The entire vagina, from the region above the introitus to the region just below the cervix was removed from the animal (Fig. 2(d)). Its hydration was maintained with phosphate buffered saline (PBS) solution throughout dissection and preparation. The specimen was carefully opened and was trimmed to be square, with sides measuring approximately 15 mm and aligned with the LD and CD (Fig. 2(e)).

2.2. Clamping and mounting system, biaxial testing system, and DIC system

In order to reduce preparation time, minimize handling, and correctly align and mount the specimen in a custom-made biaxial testing apparatus, a new clamping/mounting system was designed and fabricated in polylactic acid using a 3D printer (Replicator 2, MakerBot, New York, NY) (Fig. 3). The main components of the clamping system are a base with a central raised square platform (Fig. 3(a)), eight rectangular blocks (Fig. 3(b)) which were superglued to build four clamps with three sewing needles bent to 90° each (Fig. 3(c)), a frame with guiding rails that held the relative position of the specimen and four clamps during dismounting from the base and mounting on to the biaxial system (Fig. 3(d)), and L-shaped brackets (Fig. 3(c)) that connected the actuators of the biaxial testing system to the clamps. The top face of the raised square platform was approximately the same size of the specimens. It had a small hole in each of the four corners as well as three guiding holes, which were spaced approximately 3.5 mm from each other, along each of the four borders (Fig. 3(a)). For clamping, each specimen was laid flat, with the abluminal side of

of the raised square platform (Fig. 3(c)), were punctured through the specimen into the guiding holes. The distances between the three needles of the clamps were fixed, thus constraining the deformation of the side lengths of the specimens during testing. However, the benefits of this clamping system, especially the minimization of tissue handling and the uniform spacing of securement sites, outweighed the limitations posed by the fixed widths. The needles securing the placement of the specimen at the corners were then removed, and the frame with guiding rails (Fig. 3(d)) was placed on top of the specimen and clamps to hold their relative position. The frame, specimen, clamps, and base were gently flipped over together, and the base was removed, leaving the frame holding the clamped specimen that was now luminal side up. The clamped specimen was placed inside a fume hood and a speckle pattern was applied to its luminal side by spraying black paint (Rust-Oleum, Vernon Hills, IL) through a mesh screen (9329T511, McMaster-Carr, Elmhurst, IL) for non-contact strain measurement. The specimen was then held under a gentle flow of air from a laboratory compressed air tap for 5 to 10 seconds to help dry the paint. Once speckled, the specimen and clamps were secured to a custom-made biaxial machine by lowering the frame such that the hole on the backside of each clamp (Fig. 3(c)) was positioned onto the pegs of the L-shaped brackets (Fig. 3(e)), and the frame was removed. The custom-built planar biaxial testing apparatus was equipped with 2 load cells of 50 g capacity and 0.1% accuracy (LSB200, Futek, Irvine, CA) and 4 linear actuators (T-NA08A25, Zaber Technologies Inc., Canada) (Fig. 4(a)). Two high resolution CMOS cameras (Basler ace acA2440-75 um, Basler, Inc., Exton, PA) were mounted above the specimen to take images for length measurement and for strain analysis (Fig. 4(b)). A commercial DIC system (Vic-3D, 8, Correlated Solutions, SC) was calibrated immediately before testing each specimen using a standard calibration grid with 3 mm spacing.

The specimen was submerged in a physiologic bath solution (Krebs-Ringer bicarbonate buffer with 2 mM $CaCl_2$). A 5 mN preload was applied along both the LD and CD. This preload was chosen since it was the lowest load that consistently held the specimen such that it was not drooping, while still not being overly taut. Preconditioning was not performed in order to minimize testing time for the sake of muscle viability. The initial lengths of the tissue along the LD and CD, 1.0 L_0^{LD} and 1.0 L_0^{CD}, were considered to be the distances between the insertion points of the needles along each direction corresponding to this preloaded state (Fig. 4(a)). These distances were measured from images of the specimen taken in this configuration using ImageJ (NIH). The mean (± std. dev.) initial length along the LD was 10.01 ± 0.66 mm, and along the CD was 10.95 ± 0.86 mm. The tissue was allowed to equilibrate at these lengths for 5 minutes. Muscular contraction was induced by replacing the bath solution with a potassium stimulation solution (Krebs-Ringer bicarbonate buffer with 2 mM $CaCl_2$ and 124 mM KCl) [7,9,30]. Once the stimulation solution was added, high resolution images were taken at a frequency of 4 Hz using the commercial DIC system and the axial forces in the LD and CD were monitored and collected at a frequency of 1613 Hz using the custom-built biaxial system. Data collection and image acquisition were stopped once the force values were observed to plateau, indicating the contraction had reached its peak, which typically took between 100 and 150 seconds. The stimulation solution was removed, the specimen was gently washed, and KCl-free bath solution was returned. The specimen was then simultaneously pulled in the LD to 1.1 L_0^{LD} and in the CD to 1.1 L_0^{CD} at a displacement rate of 0.03 mm/s. The specimen was allowed to equilibrate for 5

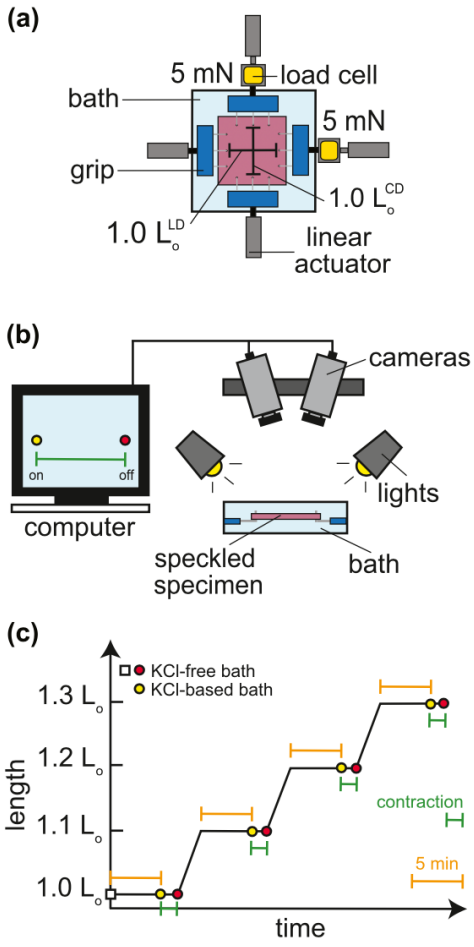

Fig. 4. (a) Specimen in the initial configuration subjected to 5 mN pre-loads along both LD and CD. (b) DIC system and cameras used to measure strains during KCl-induced contractions. (c) Displacement of the specimen along one of the two loading axes (LD or CD).

lated to contract again. This process was repeated with the specimen being stretched to lengths of 1.2 L_0 and 1.3 L_0, for a total of four stimulations. A schematic of the setup and protocol is presented in Fig. 4(b), (c).

After being contracted at each of the four equi-biaxial stretch levels, the specimen was removed from the testing apparatus, rinsed, and allowed to relax for several minutes. A CCD laser displacement sensor (Keyence, Japan) was then used to measure specimen thickness at five spots across the specimen. The average of the five thickness measurements was multiplied by its initial tissue lengths (1.0 L_0^{CD} and 1.0 L_0^{LD}) to obtain tissue volume for use in force normalization. It should be noted that the thickness used for force normalization was measured after mechanical testing to retain muscle viability. This thickness may be different than the thickness of the specimen before testing due to stretching, possible swelling, and viscoelastic effects. The average thickness of all specimens was 0.31 ± 0.04 mm, and the average volume was 33.89 ± 6.83 mm^3. Specimen volume was normally distributed and there were no outliers.

2.3. Data processing

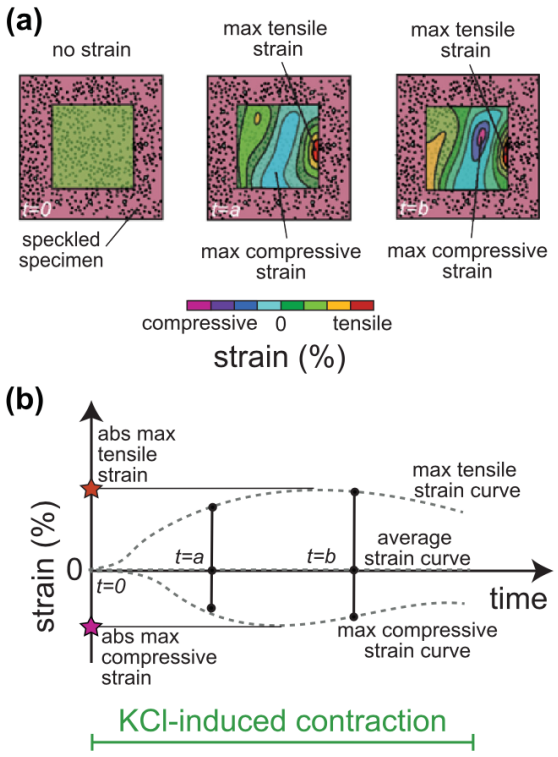

Fig. 5. (a) Schematics of strain maps for one specimen in one axial loading direction when contraction starts ($t = 0$) and at two subsequent time points ($t = a$ and $t = b$) during one KCl-induced contraction. At each time point, the maximum (max) compressive strain, the maximum tensile strain, and the average strain are calculated. Since the specimen is held fixed at an equi-biaxial stretch level, the average strain at each time point during contraction is nearly zero. (b) Maximum tensile strains, maximum compressive strains, and average strains (equal to zero) versus time collected during one KCl-induced contraction. Absolute maximum (abs max) tensile strain is the maximum (over time) of the max tensile strains (over specimen) and the absolute maximum compressive strain is the maximum (over time) of the max compressive strains (over specimen) during one KCl-induced contraction, respectively.

compressive, and average normal Lagrangian strains in the LD and CD over the central region of the specimen. For each contraction, the image that was used to define the reference configuration of the specimen for strain analysis was selected as the first image after the KCl solution had been poured into the bath, which was before the specimen started to contract and 5 minutes after the specimen had been pulled to a given equi-biaxial stretch. As such, strains reported in this study did not include the strains induced by pulling the specimen to each applied equi-biaxial stretch, but rather represented the strains that the specimen experienced due to tissue contraction.

The maximum tensile strain, maximum compressive strain, and average strain within the central region of the specimen were identified at each time point and plotted against time, as depicted in Fig. 5(a), (b). Maximum principal strains were not computed since they were found to be comparable in magnitude, although different, to the maximum normal strains. The maximum (over time) of maximum (over the specimen) tensile and compressive strains that the specimen experienced throughout the entire duration of each contraction were determined and reported as absolute maximum tensile strain and absolute maximum compressive strain, respectively (Fig. 5(b)). Only specimens for which dislodged from the specimen while pouring solutions, such as a speck of paint, which introduced errors in DIC measurements.

Contractile forces were reported for all the tested specimens in both the LD and CD. Contractile force in one axial direction was defined to be the difference between the steady-state passive force, that is, the force due to a given stretch immediately following the addition of KCl after equilibrating for 5 minutes, and the maximum force reached during the contraction at that stretch. Note that the contractile forces reported here represented the additional forces generated by VaSM in response to stimulation and did not include basal tone forces. The contractile forces of each specimen were divided by the tissue volume of that specimen to obtain contractile force normalized by volume.

2.4. Statistical analysis

Statistical analysis was performed using SPSS 27 (IBM Corp, Armonk, NY). Comparisons were considered significant when $p < 0.05$. Two-way repeated measures ANOVAs were used to determine the effect of anatomical direction and applied equi-biaxial stretch on absolute maximum (compressive or tensile) strain values. There were no outliers among the absolute maximum (compressive or tensile) strain values, as studentized residuals were between -3 and +3. Data were assessed for normality with Shapiro-Wilk's tests. Absolute maximum compressive strain data were normally distributed ($p > 0.05$) except at stretches 1.1 L_0^{LD} ($p = 0.025$) and 1.3 L_0^{LD} ($p = 0.009$). Absolute maximum tensile strain data were normally distributed ($p > 0.05$) except at stretches 1.0 L_0^{LD} ($p = 0.033$) and 1.1 L_0^{LD} ($p = 0.034$). Square root transformations were performed on the absolute maximum (compressive or tensile) strain data sets, which resulted in normally distributed data for all test groups, with no outliers. Whether or not comparisons regarding absolute maximum (compressive or tensile) strains reached significance was not affected by the use of transformed or non-transformed data, and therefore non-transformed absolute maximum strain data are presented.

Similarly, a two-way repeated measures ANOVA was used to assess the effect of anatomical direction and applied equi-biaxial stretch on contractile force normalized by specimen volume. There was 1 outlier, and contractile force data per volume were not normally distributed. A square root transformation and a $log_{10}(x+1)$ transformation were performed, however each of these transformations resulted in several test groups that were still not normally distributed and the outlier was still present. When the outlier was removed from the dataset, the data in all test groups were normally distributed except for the contractile force per volume at an applied stretch of 1.3 L_0^{CD} ($p < 0.0005$) and 1.3 L_0^{LD} ($p = 0.011$). Then, a square root transformation was applied, which resulted in data with no outliers that were normally distributed except at 1.3 L_0^{CD} ($p < 0.0005$). Whether or not comparisons reached significance was not affected by the removal of the outlier or by the use of transformed or non-transformed data, and therefore non-transformed contractile force by specimen volume data with the outlier included will be presented.

Greenhouse-Geisser corrections were applied when Mauchly's tests revealed violations against the assumption of sphericity. When statistically significant two-way interactions between anatomical direction and equi-biaxial stretch were reached, simple main effects were assessed via one-way repeated measures ANOVA tests. If there was not a significant interaction between anatomical direction and equi-biaxial stretch level, main effects were assessed. When significant main effects or significant simple main effects of

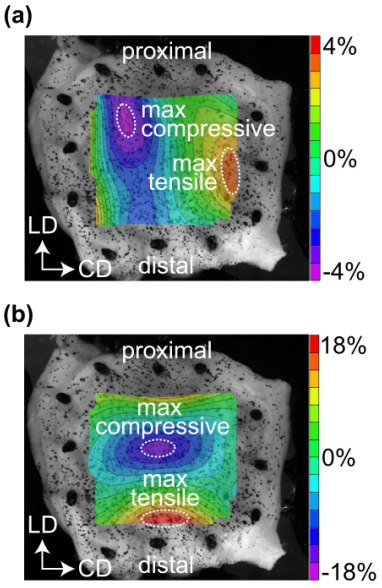

Fig. 6. Maps of (normal Lagrangian) strains in the (a) CD and (b) LD for one representative specimen 60 seconds after KCl-induced stimulation at an applied equi-biaxial stretch of 1.1 L_0. The average strains were −1.90% and −0.54% and the contractile forces were 6.57 mN and 3.44 mN in the LD and the CD, respectively.

3. Results

3.1. Contractile strain

Contractile strains were measured successfully during each of the four KCl-induced contractions for 10 of the 15 tested vaginal specimens. At any given time throughout contractions, the strain fields were highly heterogeneous across the specimens, with regions of compressive (negative) strains as well as regions of tensile (positive) strains. The average (across the specimen) strains at each time remained very small and approached zero since the outer edges of the specimens were constrained such that the overall specimen lengths were maintained at the imposed equibiaxial stretches during contractions. Vaginal specimens were usually compressed toward the proximal region, resulting in compressive strains in the proximal region and tensile strain in the distal region along the LD. The heterogeneous strain field with maximum compressive and tensile strains of one representative specimen at one time point during one contraction is shown in Fig. 6. Fig. 7 displays the maximum compressive, maximum tensile, and average strain data throughout the time of a single contraction as computed over the central region of one representative specimen. The absolute compressive and tensile strain values for this contraction are also reported (Fig. 7(a), (b)).

The absolute maximum compressive strains were found to occur in the proximal vagina for 32 of the 40 total contractions for which strain was measured, and in either the center or distal vagina for the other 8 contractions. The mean values of the absolute maximum compressive strains in both LD and CD at each applied equi-biaxial stretch are displayed in Fig. 8(a). These strain values in the CD varied by less than 1% across the applied equi-biaxial stretches (Fig. 8(a)), ranging between −2.55 ± 1.64% at 1.3 L_0 and −3.44 ± 1.93% at 1.1 L_0. The mean values of the absolute maximum compressive strains in the LD varied from −9.78

Table 1
Mean (± std. dev.) contractile forces measured in the LD and CD at four applied equibiaxial stretches from rat vaginal specimens ($n = 15$).

Contractile force (mN)		Applied equi-biaxial stretch
LD	CD	
4.61 ± 2.59	2.19 ± 1.63	1.0 L_0
6.96 ± 3.85	3.87 ± 3.56	1.1 L_0
6.89 ± 3.19	3.91 ± 4.30	1.2 L_0
6.50 ± 6.33	3.44 ± 6.50	1.3 L_0

rection and equi-biaxial stretch were assessed. The vagina experienced significantly higher absolute maximum compressive strains in the LD than in the CD at each applied equi-biaxial stretch. This difference was most pronounced at 1.2 L_0, at which there was a mean difference of 13.24% (95% CI= 6.10% – 20.38%, $p = 0.002$) between the absolute maximum compressive strain values in the two anatomical directions. There was a significant simple main effect of applied equi-biaxial stretch on absolute maximum compressive strain in the LD ($p = 0.023$), but not in the CD ($p = 0.320$) (Fig. 8(a)). Along the LD, absolute maximum compressive strain was higher at 1.1 L_0 than it was at 1.0 L_0 ($p = 0.039$), it was similar at 1.1 L_0 and 1.2 L_0, and it was lower in magnitude at 1.3 L_0 than at 1.2 L_0 ($p = 0.007$). The most extreme values of absolute compressive strains reached by any specimen at any applied equi-biaxial stretch were −7.04% in the CD and −40.84% in the LD.

Mean (± std. dev.) values of absolute maximum tensile strain at each applied stretch are displayed in Fig. 8(b). These values along the CD ranged between 2.51± 1.82% at 1.3 L_0 and 4.66 ± 3.23% at 1.0 L_0, and along the LD ranged between 6.69 ± 6.60% at 1.3 L_0 and 12.95 ± 9.05% at 1.1 L_0. There was not a significant two-way interaction between applied equi-biaxial stretch and anatomical direction on absolute maximum tensile strain ($p = 0.241$). There was a significant main effect of anatomical direction ($p = 0.007$) but not of applied equi-biaxial stretch ($p = 0.146$). The vagina experienced significantly higher absolute maximum tensile strain in the LD than in the CD, with a mean difference of 7.31% (95% CI= 2.60% to 12.01%). Finally, the most extreme values of absolute maximum tensile strains reached by any specimen at any equi-biaxial stretch were 11.33% for the CD and 36.00% for the LD.

Since the specimens were constrained along all their four sides during each contraction, compression in one area was balanced by tension in another area, resulting in very small average strains over the specimen. This is shown for one representative specimen in Fig. 7(c). The average strain for any specimen at any equibiaxial stretch was between −1% and 1% along the CD, and between −3.48% and 5.23% along the LD.

3.2. Contractile force

Force data were successfully collected for all vaginal specimens ($n = 15$), at each applied equi-biaxial stretch. Fig. 7(d) shows the force data over time for one representative specimen during one KCl-induced stimulation. Steady-state passive forces (i.e., force prior to KCl-induced stimulation) were 2.90 ± 0.64 mN, 5.92 ± 0.88 mN, 34.90 ± 7.06 mN, and 129.10 ± 23.59 in the CD and 2.48 ± 0.90 mN, 1.89 ± 0.90 mN. 21.42 ± 5.30 mN, and 99.60 ± 19.60 in the LD at equi-biaxial stretches of 1.0, 1.1, 1.2, and 1.3, respectively.

Average contractile forces in the CD ranged between 2.19 ± 1.63 mN at an equi-biaxial stretch of 1.0 and 3.91 ± 4.30 mN at an equi-biaxial stretch of 1.2 L_0, and in the LD ranged between 4.61

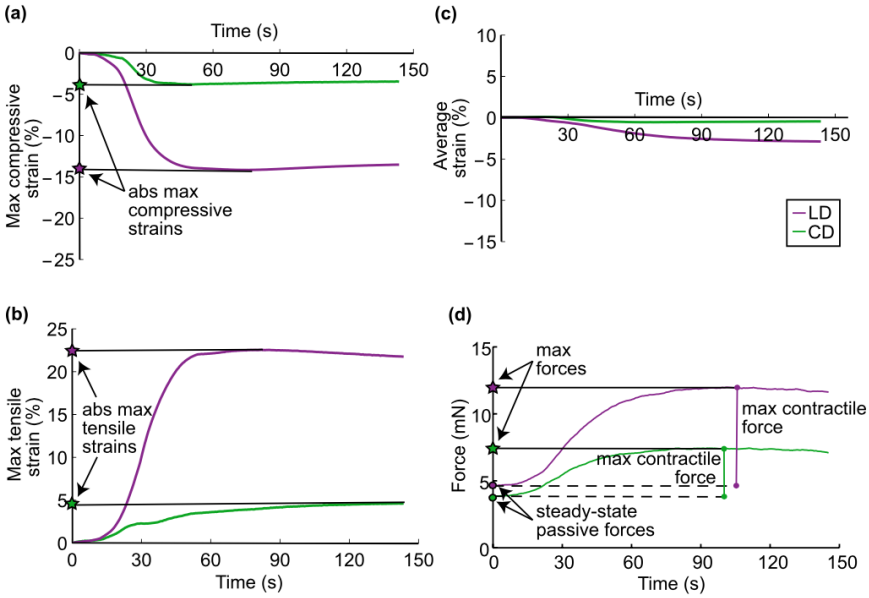

Fig. 7. (a) Maximum compressive strain, (b) maximum tensile strain, (c) average strain, and (d) force versus time in the LD and CD throughout the duration of one contraction at an applied equi-biaxial stretch of 1.1 L_0 for one representative specimen. Absolute maximum (abs max) compressive and tensile strains are reported in (a) and (b) and maximum (max) force is reported in (d). Note that the forces at $t = 0$ represent the steady-state passive forces due to the applied equi-biaxial stretch after 5 minutes of equilibration.

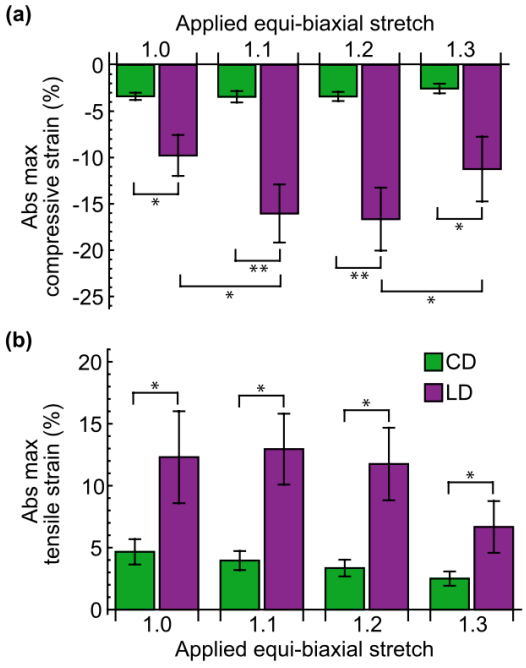

Fig. 8. Mean (±std. dev.) values of (a) absolute maximum compressive strains and (b) absolute maximum tensile strains at four applied equi-biaxial stretches (1.0, 1.1, 1.2, and 1.3) during KCl-induced contractions of vaginal specimens ($n = 10$). (* $p < 0.05$, ** $p < 0.005$)

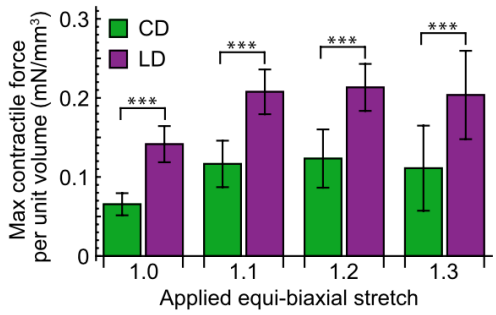

Fig. 9. Mean (±std. dev.) values of the max contractile forces that were induced by KCl normalized by the volumes of the vaginal specimens (prior to testing) at four applied equi-biaxial stretches (1.0, 1.1, 1.2, and 1.3) ($n = 15$). (*** $p < 0.0005$)

hand, only 6 specimens had non-zero contractions along the CD at 1.3 L_0.

Mean (± std. dev.) contractile force data normalized by specimen volume at each equi-biaxial stretch are reported in Fig. 9. The vagina experienced significantly higher contractile forces normalized by volume along the LD than along the CD, with a mean difference of 0.087 mN/mm^3 (95% CI=0.061 – 0.114%). The mean contractile force normalized by specimen volume ranged between 0.065 ± 0.054 mN/mm^3 at an equi-biaxial stretch of 1.0 to 0.123 ± 0.142 mN/mm^3 at an equi-biaxial stretch of 1.2 in the CD and between 0.142 ± 0.089 mN/mm^3 at an equi-biaxial stretch of 1.0 and 0.213 ± 0.115 mN/mm^3 at an equi-biaxial stretch of 1.2 in the LD.

4. Discussion

This study presents the first high-resolution *ex vivo* strain measurements of the vagina during isometric contractions. Vaginal specimens isolated from rats were stretched biaxially along the LD and CD in order to simulate the *in vivo* loading conditions of the organ. Each specimen was held at four equi-biaxial stretches and contractions were induced with a high potassium solution.

strains along the LD, in the proximal region of the vagina (Fig. 6). The vagina was found to experience significantly larger contractile strains and generate significantly larger contractile forces along the LD than along the CD (Figs. 8 and 9). To our knowledge, the full-field two-dimensional strains that are induced in the vagina by VaSM contractions had never been quantified until now. In fact, there are not many reports of full-field strain measurements of the passive vagina during mechanical tests either. Only a few experimental studies have utilized the DIC technique to evaluate full-field displacement and strain maps of passive vaginal specimens during mechanical testing [31–33].

The functional significance of VaSM remains largely unknown, though VaSM is likely important for the maintenance of vaginal tone, sexual arousal, childbirth, and pelvic organ support. The slight contraction of VaSM, known as basal tone, is important for maintaining the resting position of the vagina [10], while the relaxation of VaSM is important for sexual arousal as it results in decreased luminal pressure and increased vaginal length in preparation for intercourse [34]. The finding that during contraction the vagina strains more and generates higher forces along the LD than the CD could indicate that VaSM plays a more significant role in controlling vaginal length than in controlling vaginal diameter.

Smooth muscle contraction occurs with an increase of intracellular Ca^{2+}. Such increase leads to a cascade of events and, ultimately, to thick myosin filaments forming cross-bridges with thin actin filaments. The myosin and actin filaments slide across each other, shortening the contractile units of smooth muscle cells. The influx of Ca^{2+} into the intracellular fluid can be induced through neurotransmitter signaling; neurotransmitters bind to specific receptors which activate a series of proteins and messengers that open Ca^{2+} channels. These events have been simulated experimentally in the vagina through EFS, which causes the release of neurotransmitters from nerve terminals, and by directly adding neurotransmitters or their agonists to solutions in which the organ is immersed [30]. Hormones can also result in Ca^{2+} influx; in the vagina oxytocin has been shown to induce contractions [35]. Contractions may also occur spontaneously, without external stimulation of smooth muscle, and this has been observed in the vagina [36]. Lastly, mechanical stretch can cause contractions in some smooth muscle, such as that of the stomach [37], but this has not been reported for vaginal tissue. Very little is known about the molecular processes during the contractile activities of VaSM, including which signaling pathway is the predominant means for contraction. Here, we chose to stimulate VaSM to contract using a high concentration of KCl, which directly depolarizes the cell membrane, resulting in the opening of Ca^{2+} channels, bypassing more complex signaling pathways. The results of previous KCl sensitivity tests performed on the rat vagina by Feola et al. [41] indicate that our chosen concentration of 124 mM was well above the concentration necessary to invoke maximal contractile response.

We reported highly inhomogeneous strains across vaginal specimens during KCl-induced contractions, and we identified specific regions across the specimen where the maximum tensile and compressive strains occurred (Fig. 6). In our experimental setup and protocol, during isometric contractions, the overall side-lengths of the square specimens were not permitted to shorten or elongate as the clamps were fixed. Thus, compression due to contraction in one area of the specimen within the clamped region resulted in tension in another area. It is likely that areas that exhibited compressive strains were those in which VaSM contracted the most, while areas with tensile strains were being stretched towards the most contractile regions. If the specimens were free-floating in- any form of clamps or needles will reduce the area across which strain can be accurately measured and will create regions with stress concentration. The vagina experienced compressive strains of magnitude up to 40.84% along the LD and 7.04% along the CD, and tensile strains of magnitude up to 36.00% along the LD and 11.33% along the CD. The ability of the vagina to generate these large contraction-induced strains in addition to the strains it experienced due to external loading cannot be ignored when characterizing the overall mechanical behavior of the vagina.

The peak compressive strains typically occurred in the proximal vagina. These findings are in agreement with previous studies by Clark et al. [10] for the murine vagina, where the proximal vagina was reported to have experienced greater changes in outer diameter than the distal vagina during contractions at various intraluminal pressures and axial lengths. Along these lines, there are several published studies that demonstrated that the proximal vagina generates higher contractile forces than the distal vagina [5,8,10,38] and that there is more muscle in the proximal vagina than the distal vagina [5,8]. Together these results suggest that there is an increased effect of VaSM on the stresses and strains of the vagina in the proximal region.

In response to KCl, we found that the vagina generates higher contractile forces along the LD than along the CD, confirming previous research findings. By performing inflation-extension tests [10] and planar biaxial tests [9], respectively, KCl-induced stimulation also resulted in higher stresses generated along the LD of rodent vaginas. Several investigators have compared the contractile forces generated along the LD and CD of the vagina using uniaxial testing methods, and did not observe higher contractile forces in the LD. Giraldi et al. [7] reported higher contractile forces in tissue strips cut along the CD of rat vaginas, stating that tissue strips cut along the LD did not respond to EFS or high potassium stimulation. While this finding was supported by Onol et al. [39], several subsequent studies have observed non-zero contractile forces for tissue strips oriented along the LD of rat vaginas [5,40–42]. Oh et al. [8] also compared contractile forces of the rabbit vagina in the LD and CD using uniaxial tensile testing, and found no statistical difference in these forces between the two directions. The discrepancies between findings from biaxial testing and uniaxial testing regarding direction-dependent differences in contractile forces may point to important coupling effects between the two anatomical directions of the vagina. These differences could also be a result of the size of tissue specimens used in experiments; in inflation-extension and planar biaxial tests, whole vaginas were tested, whereas in uniaxial tests only strips of tissue were tested. The exact anatomical region from which strips were isolated likely has a large impact on the measured contractile properties.

The relative quantity of smooth muscle oriented along the LD compared to the CD has not been determined even though it likely contributes to the direction-dependent contractile properties of the vaginal tissue. Since potassium stimulates muscle non-selectively, recent findings that the tissue contracts more in the LD than the CD in response to KCl [9,10] could indicate that there is a larger quantity of VaSM oriented longitudinally, at least in rodents. Quantitative histological analysis should be performed in future studies to determine the orientation of VaSM so that the mechanical function of vaginal tissue can be related to its micro-structure. There could also be differences in the properties of the CD and LD oriented muscle cells themselves. In the guinea pig stomach [43] and the rabbit rectum [44], differences were observed between the contractility of LD and CD oriented smooth muscle; it was hypothesized that this was due to differences in calcium storage mecha-

ported) showed that contractile forces were consistently lower at 1.3 than at 1.2, indicating that at 1.3 we had exceeded the optimal stretch at which maximal contractions are generated. Here, on average the greatest contractile forces were generated at an applied stretch of 1.2 along both anatomical directions, though there was not a statistically significant main effect of stretch on contractile force. Contractile strains along the LD tended to be larger in magnitude at applied stretches of 1.1 and 1.2 than at 1.0 and 1.3, but strains along the CD were similar across all stretches, for the most part (Fig. 8). Only 6 out of 15 specimens generated contractile force along the CD at an equi-biaxial stretch of 1.3, whereas 14 of 15 specimens generated contractile force at this stretch along the LD. This could indicate that the vagina has a wider range of stretches at which contractions can be generated in the LD than the CD. However, it is also possible that these decreased contractile forces could be the result of interference of measurement due to specimen relaxation. Forces along the CD and LD increased while pulling the specimens to a given applied equi-biaxial stretch. Once the appropriate length was reached and the actuators halted, these forces began to decrease as the specimen relaxed. Five minute equilibration periods were included prior to contraction at each applied equi-biaxial stretch to give the specimen time to reach equilibrium so that decreases in force associated with relaxation would not interfere with recording increases in force due to contraction. If specimens were still relaxing even a little after the 5 minute period, it would reduce the apparent magnitude of contractile force.

The majority of vaginal contractile studies have been performed in 37°C baths, with two exceptions [8,9] which were both performed at room temperature. We performed our testing at room temperature without oxygenation. We expect minimal effect of these factors due to the short time scale of the experiment; the time between the animal euthanasia and the end of an experiment was between 40 and 60 minutes. Despite the differences in bath temperature and oxygenation, the contractile forces normalized by specimen volume along the LD and CD obtained in this study (Fig. 9) fell within and just below, respectively, the range of contractile values reported in other studies, which were summarized in our recent review [15]. Lastly, like many other vaginal contractile studies [15], the estrous phase of the rats was not considered in this study. Estrous cycle has not been observed to correlate with differences in contractile functionality in rats [7,30], though this has not been confirmed with large-scale studies.

Throughout this study, one of the main challenges we faced was speckle pattern degradation, resulting in loss of strain data for several specimens (33% of the tested specimens). We found that placing the speckled surface of the specimen under a very gentle air flow for just a few seconds reduced the number of speckles that floated off of the specimen once submerged for testing. Because we wanted to minimize tissue drying and retain muscle viability, we did not allow the spray paint to fully dry and adhere to the specimens. Future investigators who wish to use the DIC technique to study the contractile properties of biological tissues should consider alternative methods for creating speckle patterns so as to maximize the success of their strain analysis.

The functionality and morphology of VaSM are compromised with the development of POP and, as several studies pointed out, with mesh devices that are used for POP surgical treatment. Mesh implants have several detrimental effects on the VaSM health including thinning of the muscularis layer [28], reduction in size and loss of organization of muscle bundles [26], and decrease in contractile force generation [24–28]. We have quantified the large gators reported the presence of residual strains in murine vaginal tissue [45] which may alter the *in vivo* contractions of VaSM. For this reason, more physiologically relevant loading conditions must be considered to fully determine the strains induced in the vagina by contractions. Ideally, these strains should be measured *in vivo*, where the vagina is likely not subjected to equi-biaxial stretching. Here, we selected the equi-biaxial stretching conditions since we wanted to measure differences in strains between the LD and CD solely due to micro-structural differences. If one were to apply non-equibiaxial stretching, then the eventual differences in strains between LD and CD - would be a bit harder to interpret since it could be due to both applied non equi-biaxial stretching and vaginal microstructure. That said, if the findings presented here hold true also for the more complex *in vivo* loading conditions, the inhomogeneous strain fields of the vagina induced by contractions and the differences in strains between the LD and CD will need to be considered when designing vaginal mesh devices. These devices must be able to sustain strains as large as those that - are experienced by the native vaginal tissue.

Despite the obvious anatomical differences between the rat and the human, the rat remains the most preeminent animal model for studies on the mechanical properties of the vagina. The human and rat vaginas are both described as having similar layered structure with the epithelium, muscularis, and adventitia layers [46,47]. More specifically, both human and rat vaginas contain circumferentially and longitudinally oriented VaSM in the muscularis [5,46] and, for this reason, the active mechanical behavior of the vagina is expected to be similar in the two species. The rat vagina is described as being supported by comparable structures as the human vagina within the pelvic cavity [47]. That said, comparative studies are needed to determine how the results presented here can be translated to humans in order to understand the etiology of PFDs, POP, and develop better prevention and treatment methods.

5. Conclusions

KCl-induced contractions of smooth muscle within the vagina at fixed equi-biaxial stretches generated highly inhomogeneous strain fields, with strains in the LD significantly higher than those in the CD. Similarly, higher contractile forces were generated along the LD than along the CD. The functional significance of longitudinally oriented muscle in the vagina remains unknown, but the seemingly dominant contractility of the vagina along the LD could indicate that it is important for sexual function or pelvic support. The ability of the vagina to induce stress and strain via contractions is a crucial component of its overall mechanical behavior and needs to be considered when developing new treatments for PFDs including mesh materials for use as vaginal support.

Funding data

Funding was provided by NSF Grant No. 1804432 and NSF Grant No. 1929731.

Declaration of Competing Interest

The authors declare that they have no known competing financial interests or personal relationships that could have appeared to influence the work reported in this paper.

CRediT authorship contribution statement

Abramowitch: Conceptualization, Formal analysis, Writing - review & editing. **Pamela A. Moalli:** Conceptualization, Formal analysis, Writing - review & editing. **Raffaella De Vita:** Conceptualization, Investigation, Methodology, Data curation, Formal analysis, Visualization, Writing - original draft, Writing - review & editing, Resources, Funding acquisition, Project administration, Supervision.

References

[1] M. Farage, H. Maibach, Lifetime changes in the vulva and vagina, Arch. Gynecol. Obstet. 273 (4) (2006) 195–202.
[2] R.J. Levin, Recreaion and procreation: A critical view of sex in the human female, Clin. Anat. 28 (3) (2015) 339–354.
[3] K.T. Barnhart, E.S. Pretorius, D. Malamud, Lesson learned and dispelled myths: Three-dimensional imaging of the human vagina, Fertil. Steril. 81 (5) (2004) 1383–1384.
[4] K.T. Barnhart, A. Izquierdo, E.S. Pretorius, D.M. Shera, M. Shabbout, A. Shaunik, Baseline dimensions of the human vagina, Hum. Reprod. 21 (6) (2006) 1618–1622.
[5] M. Basha, S. Chang, E.M. Smolock, R.S. Moreland, A.J. Wein, S. Chacko, Regional differences in myosin heavy chain isoform expression and maximal shortening velocity of the rat vaginal wall smooth muscle, Am. J. Physiol. Regul. Integr. Comp. Physiol. 291 (4) (2006). R1076–R1084
[6] M.K. Boreham, C.Y. Wai, R.T. Miller, J.I. Schaffer, R.A. Word, Morphometric properties of the posterior vaginal wall in women with pelvic organ prolapse, Am. J. Obstet. Gynecol. 187 (6) (2002) 1501–1509.
[7] A. Giraldi, P. Alm, V. Werkström, L. Myllymäki, G. Wagner, K.E. Andersson, Morphological and functional characterization of a rat vaginal smooth muscle sphincter, Int. J. Impot. Res. 14 (4) (2002) 271–282.
[8] S.-J. Oh, S.K. Hong, S. Kim, J. Paick, Histological and functional aspects of different regions of the rabbit vagina, Int. J. Impot. Res. 15 (2) (2003) 142–150.
[9] A. Huntington, E. Rizzuto, S. Abramowitch, Z.D. Prete, R. De Vita, Anisotropy of the passive and active rat vagina under biaxial loading, Ann. Biomed. Eng. 47 (1) (2019) 272–281.
[10] G.L. Clark, A.P. Pokutta-Paskaleva, D.J. Lawrence, S.H. Lindsey, L. Desrosiers, L.R. Knoepp, C.L. Bayer, R.L. Gleason Jr, K.S. Miller, Smooth muscle regional contribution to vaginal wall function, Interface Focus 9 (4) (2019) 20190025.
[11] M. Borsdorf, A. Tomalka, N. Stutzig, E. Morales-Orcajo, M. Böl, T. Siebert, Locational and directional dependencies of smooth muscle properties in pig urinary bladder, Front. Physiol. 10 (2019) 63.
[12] M. Bauer, E. Morales-Orcajo, L. Klemm, R. Seydewitz, V. Fiebach, T. Siebert, M. Böl, Biomechanical and microstructural characterisation of the porcine stomach wall: Location-and layer-dependent investigations, Acta Biomater. 102 (2020) 83–99.
[13] L.C. Skoczylas, Z. Jallah, Y. Sugino, S.E. Stein, A. Feola, N. Yoshimura, P. Moalli, Regional differences in rat vaginal smooth muscle contractility and morphology, Reprod. Sci. 20 (4) (2013) 382–390.
[14] I. Urbankova, G. Callewaert, S. Blacher, D. Deprest, L. Hympanova, A. Feola, L. De Landsheere, J. Deprest, First delivery and ovariectomy affect biomechanical and structural properties of the vagina in the ovine model, Int. Urogynecol. J. 30 (3) (2019) 455–464.
[15] A. Huntington, K. Donaldson, R. De Vita, Contractile properties of vaginal tissue, J. Biomech. Eng. 142 (8) (2020) 080801.
[16] I. Nygaard, M.D. Barber, K.L. Burgio, K. Kenton, S. Meikle, J. Schaffer, C. Spino, W.E. Whitehead, J. Wu, D.J. Brody, et al., Prevalence of symptomatic pelvic floor disorders in us women, Jama 300 (11) (2008) 1311–1316.
[17] J.M. Wu, C.A. Matthews, M.M. Conover, V. Pate, M.J. Funk, Lifetime risk of stress incontinence or pelvic organ prolapse surgery, Obstet. Gynaecol. 123 (6) (2014) 1201–1206.
[18] W. Badiou, G. Granier, P.-J. Bousquet, X. Monrozies, P. Mares, R. de Tayrac, Comparative histological analysis of anterior vaginal wall in women with pelvic organ prolapse or control subjects. a pilot study, Int. Urogynecol. J. 19 (5) (2008) 723–729.
[19] M.K. Boreham, C.Y. Wai, R.T. Miller, J.I. Schaffer, R.A. Word, Morphometric analysis of smooth muscle in the anterior vaginal wall of women with pelvic organ prolapse, Am. J. Obstet. Gynecol. 187 (1) (2002) 56–63.
[20] G.M. Northington, M. Basha, L.A. Arya, A.J. Wein, S. Chacko, Contractile response of human anterior vaginal muscularis in women with and without pelvic organ prolapse, Reprod. Sci. 18 (3) (2011) 296–303.
[21] P. Takacs, M. Gualtieri, M. Nassiri, K. Candiotti, C.A. Medina, Vaginal smooth muscle cell apoptosis is increased in women with pelvic organ prolapse, Int. Urogynecol. J. 19 (11) (2008) 1559–1564.
[22] M.K. Boreham, R.T. Miller, J.I. Schaffer, R.A. Word, Smooth muscle myosin heavy chain and caldesmon expression in the anterior vaginal wall of women with and without pelvic organ prolapse, Am. J. Obstet. Gynecol. 185 (4) (2001) 944–952.
[23] E. Holt, US FDA rules manufacturers to stop selling mesh devices, Lancet 393 (10182) (2019) 1686.
[24] A. Feola, S. Abramowitch, Z. Jallah, S. Stein, W. Barone, S. Palcsey, P. Moalli, Deterioration in biomechanical properties of the vagina following implantation of a high-stiffness prolapse mesh, Br. J. Obstet. Gynaecol. 120 (2) (2013) 224–232.
[25] Z. Jallah, R. Liang, A. Feola, W. Barone, S. Palcsey, S. Abramowitch, N. Yoshimura, P. Moalli, The impact of prolapse mesh on vaginal smooth muscle structure and function, Br. J. Obstet. Gynaecol. 123 (7) (2016) 1076–1085.
[26] R.M. Shaffer, R. Liang, K. Knight, C.M. Carter-Brooks, S. Abramowitch, P.A. Moalli, Impact of polypropylene prolapse mesh on vaginal smooth muscle in rhesus macaque, Am. J. Obstet. Gynecol. (2019). 330.e1-330.e9
[27] A. Feola, M. Endo, I. Urbankova, J. Vlacil, T. Deprest, S. Bettin, B. Klosterhalfen, J. Deprest, Host reaction to vaginally inserted collagen containing polypropylene implants in sheep, Am. J. Obstet. Gynecol. 212 (4) (2015). 474.e1-474e8
[28] K.M. Knight, A.M. Artsen, M.R. Routzong, G.E. King, S.D. Abramowitch, P.A. Moalli, New zealand white rabbit: a novel model for prolapse mesh implantation via a lumbar colpopexy, Int. Urogynecol. J. (2019) 1–9.
[29] R. Liang, S. Abramowitch, K. Knight, S. Palcsey, A. Nolfi, A. Feola, S. Stein, P.A. Moalli, Vaginal degeneration following implantation of synthetic mesh with increased stiffness, BJOG 120 (2) (2013) 233–243.
[30] A. Giraldi, K. Persson, V. Werkström, P. Alm, G. Wagner, K. Andersson, Effects of diabetes on neurotransmission in rat vaginal smooth muscle, Int. J. Impot. Res. 13 (2) (2001) 58–66.
[31] J.A. McGuire, C.L. Crandall, S.D. Abramowitch, R. De Vita, Inflation and rupture of vaginal tissue, Interface Focus 9 (4) (2019) 20190029.
[32] J.A. McGuire, S.D. Abramowitch, S. Maiti, R. De Vita, Swine vagina under planar biaxial loads: An investigation of large deformations and tears, J. Biomech. Eng. 141 (4) (2019) 041003.
[33] E. Pack, J. Dubik, W. Snyder, A. Simon, S. Clark, R. De Vita, Biaxial stress relaxation of vaginal tissue in pubertal gilts, J. Biomech. Eng. 142 (3) (2020) 031002.
[34] K. Park, I. Goldstein, C. Andry, M. Siroky, R. Krane, K. Azadzoi, Vasculogenic female sexual dysfunction: the hemodynamic basis for vaginal engorgement insufficiency and clitoral erectile insufficiency, Int. J. Impot. Res. 9 (1) (1997) 27–37.
[35] F.S. Gravina, D.F. van Helden, K.P. Kerr, R.B. de Oliveira, P. Jobling, Phasic contractions of the mouse vagina and cervix at different phases of the estrus cycle and during late pregnancy, PLoS One 9 (10) (2014). E111307
[36] X. Fu, H. Siltberg, P. Johnson, U. Ulmsten, Viscoelastic properties and muscular function of the human anterior vaginal wall, Int. Urogynecol. J. 6 (4) (1995) 229–234.
[37] M.T. Kirber, J.V. Walsh, J.J. Singer, Stretch-activated ion channels in smooth muscle: A mechanism for the initiation of stretch-induced contraction, Pflügers Arch. 412 (4) (1988) 339–345.
[38] D.F. van Helden, A. Kamiya, S. Kelsey, D.R. Laver, P. Jobling, R. Mitsui, H. Hashitani, Nerve-induced responses of mouse vaginal smooth muscle, Pflügers Arch. 469 (10) (2017) 373–1385.
[39] F.F. Önol, F. Ercan, T. Tarcan, The effect of ovariectomy on rat vaginal tissue contractility and histomorphology, J. Sex. Med. 3 (2) (2006) 233–241.
[40] M. Basha, E.F. LaBelle, G.M. Northington, T. Wang, A.J. Wein, S. Chacko, Functional significance of muscarinic receptor expression within the proximal and distal rat vagina, Am. J. Physiol. Regul. Integr. Comp. Physiol. 297 (5) (2009). R1486–R1493
[41] A. Feola, P. Moalli, M. Alperin, R. Duerr, R.E. Gandley, S. Abramowitch, Impact of pregnancy and vaginal delivery on the passive and active mechanics of the rat vagina, Ann. Biomed. Eng. 39 (1) (2011) 549–558.
[42] M.E. Basha, S. Chang, L.J. Burrows, J. Lassmann, A.J. Wein, R.S. Moreland, S. Chacko, Effect of estrogen on molecular and functional characteristics of the rodent vaginal muscularis, J. Sex. Med. 10 (5) (2013) 1219–1230.
[43] H. Kuriyama, K. Mishima, H. Suzuki, Some differences in contractile responses of isolated longitudinal and circular muscle from the guinea-pig stomach, J. Physiol. 251 (2) (1975) 317–331.
[44] H. Suzuki, M. Kamata, S. Kitano, H. Kuriyama, Differences in electrical properties of longitudinal and circular muscle cells of the rabbit rectum, Gen. Pharmacol. Vasc. S. 10 (6) (1979) 511–519.
[45] D.J. Capone, G.L. Clark, D. Bivona, B.O. Ogola, L. Desrosiers, L.R. Knoepp, S.H. Lindsey, K.S. Miller, Evaluating residual strain throughout the murine female reproductive system, J. Biomech. 82 (2019) 299–306.
[46] R.V. Krstic, Human microscopic anatomy: An atlas for students of medicine and biology, Springer Science & Business Media (1991).
[47] P.A. Moalli, N.S. Howden, J.L. Lowder, J. Navarro, K.M. Debes, S.D. Abramowitch, S.L. Woo, A rat model to study the structural properties of the vagina and its supportive tissues, Am. J. Obstet. Gynecol. 192 (1) (2005) 80–88.

10